Heat Capacities of Tetracene and Pentacene

Michal Fulem,*,†,‡,§ Václav Laštovka,†,‡ Martin Straka,‡ Květoslav Růžička,‡ and John M. Shaw*,†

Department of Chemical and Materials Engineering, University of Alberta, Edmonton, Alberta, T6G 2G6, Canada, Department of Physical Chemistry, Institute of Chemical Technology, Technická 5, CZ-166 28 Prague 6, Czech Republic, and Department of Semiconductors, Institute of Physics, Academy of Sciences of the Czech Republic, v. v. i., Cukrovarnická 10, 162 00 Prague 6, Czech Republic

New solid state heat capacity data for tetracene and pentacene are reported in the temperature range (258 to 600) K. The heat capacity measurements were performed using the step method with a Setaram Micro DSC III calorimeter (Institute of Chemical Technology, Prague) and a Setaram TG-DSC 111 (University of Alberta) calorimeter. These new heat capacity data are shown to be in good agreement with one another and with several solid state constant-pressure heat capacity estimation methods and quantum mechanical calculations. The new results highlight errors in the solid state heat capacity and melting point databases for polynuclear aromatic hydrocarbons.

Introduction

Interest in the thermophysical properties of pure polynuclear aromatic hydrocarbons (PAHs) has been spurred as thermodynamic property models for heavy oils and bitumen have begun to develop. This has arisen because even though diverse average molecular structures have been proposed for these complex hydrocarbon mixtures,[1,2] there is broad agreement that large PAH and mixed naphthenic PAH subunits are key constituents of their molecular structure.

Moreover, thin films of planar aromatic molecules have attracted great interest due to their potential application in thin film electronic devices. Tetracene, comprising four fused benzene rings, is used as an organic semiconductor in organic field-effect transistors (OFETs) and organic light-emitting diodes (OLEDs). Pentacene, comprising five fused benzene rings, is a promising semiconductor candidate for use in field-effect transistor technology.

In 2005, Sallamie and Shaw[3] developed a predictive technique employing density functional theory (DFT) combined with the Debye−Einstein model to compute solid state heat capacities at constant pressure, $C_p^{(s)}$, for PAHs from 0 K to their fusion temperature. In their work, an inconsistency between predicted and experimental $C_p^{(s)}$ values for tetracene was reported. On further research, we found that highly accurate quantitative structure−property relationship (QSPR) models for $C_p^{(s)}$ overpredicted available experimental heat capacity data for tetracene,[4] while predicted $C_p^{(s)}$ values for lower linear PAHs such as naphthalene and anthracene and PAHs with other geometries agreed well with experimental data. Concern arose regarding the reliability of prediction of $C_p^{(s)}$ values for larger linear PAHs such as pentacene and hexacene where data are not available in all temperature regions of interest.

Until now, it was not clear whether the published vibration frequencies or experimental $C_p^{(s)}$ for tetracene or the available QSPR predictive methods were incorrect. In the first phase of our investigation, new vibration spectra for tetracene and pentacene were measured and successfully compared with spectra obtained from DFT calculations.[5] New experimental $C_p^{(s)}$ measurements comprise the second phase of the investigation. Experimental measurements reported here were preformed on the same samples independently at two laboratories equipped with different DSC calorimeters. Comparisons between the new experimental data, the available published data, and prediction techniques are also presented. These new results highlight errors in the solid state heat capacity and melting point databases for polynuclear aromatic hydrocarbons.

Solid State Heat Capacity Prediction Methods

Three schemes for the prediction of solid heat capacity of tetracene and pentacene were considered. The first involves the use of group contribution methods, and the second employs a predictive semiempirical correlation. For the third scheme, we performed DFT calculations for tetracene and pentacene followed by the application of the method of Sallamie and Shaw.[3] A brief description of these methods is given below.

Group Contribution Methods. Domalski and Hearing[6] developed a method based on a second-order additivity scheme proposed by Benson and Buss[7] for ideal gases, to predict the solid heat capacities of organic compounds at 298.15 K. Another second-order additivity method applicable at 298.15 K used in this study was developed by Richard and Helgeson.[8] This latter method was developed especially for the estimation of $C_p^{(s)}$ of heavy hydrocarbons present in fossil fuels. Chickos et al.[9] reported a first-order group additivity scheme for estimation of heat capacity values at 298 K. Goodman et al.[10] presented two methods for the estimation of $C_p^{(s)}$ of organic compounds applicable to two temperature regions. Both methods utilize functional group definitions similar to those used in the Joback method[11] for boiling points. The first method (Goodman Power Law, GPL) employs a power law functional form for the temperature dependence of the heat capacity and is applicable from (50 to 250) K. The second method (Goodman Partition Function, GPF), applicable for temperatures above 250 K, is based on the Einstein−Debye partition function. It is more

* Corresponding authors. E-mail: michal.fulem@vscht.cz; jmshaw@ualberta.ca.
† University of Alberta.
‡ Institute of Chemical Technology.
§ Academy of Sciences of the Czech Republic.

10.1021/je800382b CCC: $40.75
Published on Web 08/16/2008

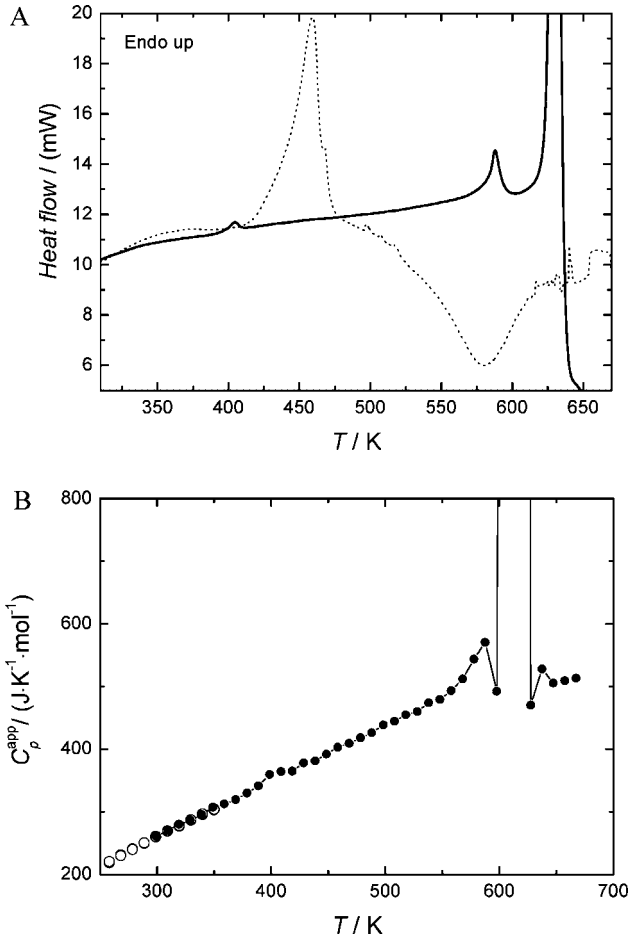

Figure 1. (A) DSC thermogram for tetracene. —, first run; ···, second run with the same sample. (B) Apparent heat capacity C_p^{app} for tetracene obtained by the step method. ○, Micro DSC III; -●-, TG-DSC 111.

complicated than the first one and requires the radius of gyration of a molecule.

Predictive Semiempirical Correlation. Laštovka and Shaw[12] developed a simple and predictive solid state heat capacity correlation based solely on the elemental composition of the solid. The correlation provides adequate estimates for pure organic compounds and is recommended in particular for larger molecules and for molecular structures not covered by other group contribution methods. The correlation has also been demonstrated to provide superb $C_p^{(s)}$ estimates for poorly defined mixed organic solids such as asphaltenes and heavy oil fractions and can be used as a phase transition identification tool for these materials.[13] The correlation has been validated for temperatures as low as 50 K. The upper temperature limit for the correlation is given by the maximum observed solid state heat capacity value of 2.5 J·K^{-1}·g^{-1}.

Prediction Based on Quantum-Mechanical Calculations. The method of Sallamie and Shaw[3] provides direct insights into the prediction of solid state heat capacities at constant pressure and is based on quantum-mechanical calculations in combination with theories by Debye and Einstein. In the first step, the heat capacity at constant volume, $C_V^{(s)}$, is calculated as the sum of contributions from atomic vibrations computed using DFT (Einstein term), which are negligible at low temperatures, and from lattice vibrations (Debye term), which asymptotically approach a constant value at high temperatures. It was found that setting the Debye temperature at 125 K provides good approximations for planar polynuclear aromatic molecules. Quantum-mechanical calculations were performed using the Gaussian software package.[14] The ground-state molecular structures were determined by complete geometry optimization using B3-LYP Hybrid DFT (Becke's three-parameter exchange functional[15] and Lee, Yang, and Parr's correlation functional[16] and the polarized 6-311G basis set). Frequency spectra calculations were performed for the optimized structures using B3 LYP/6-311G. This computational approach is in good agreement with experimental spectra.[5] It should also be noted that this approach is computationally intensive. In the second step, the difference between $C_V^{(s)}$ and $C_p^{(s)}$ is determined. For cases where sublimation pressure and density data are not available, Sallamie and Shaw[3] suggested approximate procedures based on melting point temperature. In general, $C_p^{(s)}$ is larger than $C_V^{(s)}$.

Experimental Section

Materials. Tetracene ($C_{18}H_{12}$, CASRN 92-24-0) and pentacene ($C_{22}H_{14}$, CASRN 135-48-8) were purchased from Sigma-Aldrich and were used as received. The mole fraction purities of tetracene and pentacene were $x = 0.993$ (determined by HPLC) and $x = 0.999$ (determined by GC/MS), respectively, as stated in the certificates of analysis provided by the supplier. The samples were kept under a dry nitrogen or argon atmosphere when filling the calorimeter cells.

Calorimetric Measurements. The Micro DSC III calorimeter (Setaram, France) was used for the heat capacity determination in the temperature range (258 to 350) K. The experiments with the Micro DSC III calorimeter were performed at the Institute of Chemical Technology, Prague. The measurements were carried out in the incremental temperature scanning mode (step method)[17] with a number of 10 K steps and a heating rate of 0.5 K·min^{-1} followed by isothermal delays of 3600 s. The typical mass of samples was 0.5 g. The uncertainty of heat capacity measurements performed using the step method is estimated to be less than 1 %. A detailed description of the calorimeter and calibration can be found in a recent paper by Straka et al.[18]

The heat capacity measurements in the temperature range (300 to 767) K were performed with the TG-DSC 111 (Setaram, France) at the University of Alberta, Edmonton. This calorimeter is a heat flux DSC, operating on the Tian-Calvet principle and using a cylinder-type measuring system comprising two cylindrical tubes set parallel and symmetrically in the heating furnace. The Tian-Calvet-type fluxmetric transducer (thermopile) envelopes the sample and is therefore capable of measuring almost all energy exchanges between the vessel and the unit. The TG-DSC 111 calorimeter was calibrated following recommendations developed by the working group "Calibration of Scanning Calorimeters" of the German Society of Thermal Analysis (GEFTA).[19−22] Temperature calibration to ITS 90 was performed using indium (NIST Standard reference material (SRM) 2232), tin (NIST SRM 2220), lead, and aluminum. Energy calibration was performed using the Joule effect method in the factory and checked by measuring the heat of fusion, $\Delta_{fus}H_m$, of naphthalene, a primary reference material for $\Delta_{fus}H_m$ measurements recommended by ICTAC,[23] and phenanthrene. The agreement with recommended/literature values[23−25] was within 2 %. Heat capacity calibration was performed using naphthalene, a secondary reference material for C_p measurements recommended by ICTAC.[23] The uncertainty of C_p measurements using the step method was estimated to be less than 2 %. The measurements of tetracene and pentacene were carried out using the step method with a number of 10 K steps and heating rate of 1 K·min^{-1} followed by isothermal delays

Table 1. Temperatures and Enthalpies of Phase Transitions for Tetracene[a]

	crystal III to crystal II		crystal II to crystal I		crystal I to liquid	
ref	T/K	ΔH_m/(kJ·mol^{-1})	T/K	ΔH_m/(kJ·mol^{-1})	T/K	ΔH_m/(kJ·mol^{-1})
this work	398.1 ± 1.2	0.11 ± 0.05	581.9 ± 0.5	1.2 ± 0.1	626.2 ± 0.1	36.8 ± 0.4
34	NA	NA	581.4	1.0	623.2	35.9
35	NA	NA	NA	NA	630	NA

[a] NA stands for not available.

Table 2. Experimental Isobaric Molar Heat Capacities, C_p, for Tetracene and Pentacene

Tetracene

Micro DSC III				TG-DSC 111			
T/K	C_p/(J·K^{-1}·mol^{-1})	T/K	C_p/(J·K^{-1}·mol^{-1})	T/K	C_p/(J·K^{-1}·mol^{-1})	T/K	C_p/(J·K^{-1}·mol^{-1})
crystal III		crystal III		crystal III		crystal II	
258.1	218.8	309.1	269.0	299.3	260.9	438.5	383.5
258.1	220.8	309.1	269.8	309.3	270.1	448.5	391.9
258.1	220.8	309.1	269.5	319.2	280.1	448.5	392.5
258.1	219.3	319.4	277.1	329.1	286.4	458.4	403.0
268.3	231.3	319.4	277.8	339.1	295.8	458.4	403.0
268.3	230.4	319.4	278.1	349.0	307.1	468.4	409.4
268.3	230.0	319.4	278.0	349.0	303.7	468.4	411.7
268.3	230.5	329.6	286.5	359.0	312.4	478.3	417.9
278.5	240.9	329.6	287.2	359.0	314.7	488.2	426.2
278.5	240.3	329.6	287.1	368.9	319.7	498.2	438.5
278.5	240.6	329.6	287.0	368.9	324.2	508.1	444.3
278.5	239.9	339.8	296.6	378.9	330.2	518.1	454.5
288.7	250.6	339.8	295.5	378.9	332.5	528.0	459.9
288.7	250.4	339.8	295.4	388.8	341.4	538.0	474.1
288.7	250.2	339.8	296.6	crystal II		547.9	479.3
288.7	249.7	350.0	304.4	408.7	357.6	557.8	493.4
298.9	261.0	350.0	304.2	418.6	364.9	liquid	
298.9	260.8	350.0	302.9	418.6	365.7	647.32	505.18[a]
298.9	260.5	350.0	304.1	428.6	378.1	657.27	509.31[a]
298.9	259.7			428.6	378.1	667.21	513.42[a]
309.1	269.7			438.5	381.3		

Pentacene

Micro DSC III				TG-DSC 111			
T/K	C_p/(J·K^{-1}·mol^{-1})	T/K	C_p/(J·K^{-1}·mol^{-1})	T/K	C_p/(J·K^{-1}·mol^{-1})	T/K	C_p/(J·K^{-1}·mol^{-1})
crystal		crystal		crystal		crystal	
258.1	264.5	309.1	322.1	309.2	324.4	488.2	501.9
258.1	265.5	309.1	322.4	319.2	338.9	498.2	509.1
258.1	267.2	309.1	322.3	359.0	384.6	508.1	518.2
268.3	275.7	319.4	332.5	368.9	394.9	518.1	527.8
268.3	277.2	319.4	333.2	378.9	406.0	528.0	529.1
268.3	277.1	319.4	332.1	388.8	411.4	537.9	549.1
278.5	288.9	329.6	345.7	398.7	427.1	547.9	552.3
278.5	287.1	329.6	346.5	408.7	425.7	557.8	558.6
278.5	287.5	329.6	344.5	418.6	436.8	567.8	566.7
288.7	299.7	339.8	356.2	428.6	450.1	577.7	575.7
288.7	299.7	339.8	354.9	438.5	457.6	587.7	578.8
288.7	299.2	339.8	355.1	448.5	466.7	597.6	592.5
298.9	311.6	350.0	365.5	458.4	476.5		
298.9	311.5	350.0	367.2	468.3	481.6		
298.9	311.0	350.0	366.0	478.3	497.2		

[a] Tetracene decomposes on melting.

of 1200 s. The typical mass of samples used was about 0.05 g. The hermetically sealed cells with nickel (the maximum pressure of 10 MPa at 1073 K) or aluminum sealing (the maximum pressure of 10 MPa at 573 K, the maximum temperature of 773 K) were utilized in all experiments. The tightness of the cells was checked after each experiment. No mass loss was detected.

Three successive runs were performed to obtain heat capacity of tetracene and pentacene. The measuring cell was empty in the first run and filled with the reference material and the measured sample in the second and third runs, respectively. Synthetic sapphire, NIST SRM 720, was used as the reference material. The reference cell was empty during all runs. Heat capacity was calculated from the equation

$$c_{sat,s} = \frac{m_{sapp} c_{p,sapp} (A_s - A_E)}{m_s (A_{sapp} - A_E)} \quad (1)$$

where $c_{sat,s}$ is the saturation specific heat capacity of the measured sample; $c_{p,sapp}$ is the specific heat capacity of the reference substance (synthetic sapphire); m_s is the mass of

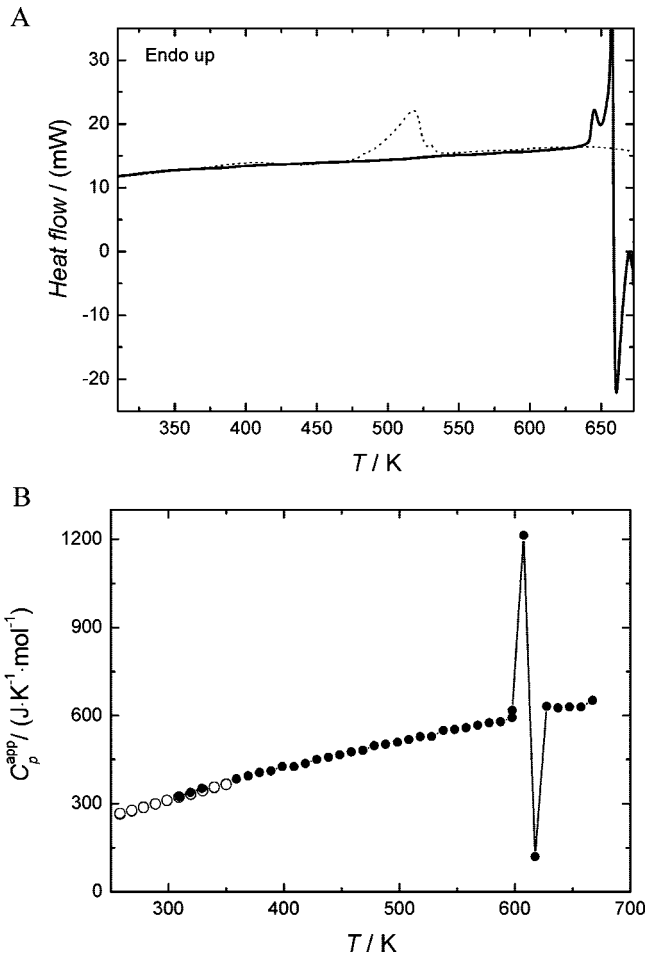

Figure 2. (A) DSC thermogram for pentacene. —, first run; ···, second run with the same sample. (B) Apparent heat capacity for pentacene C_p^{app} obtained by the step method. ○, Micro DSC III; -●-, TG-DSC 111.

the sample; m_{sapp} is the mass of the reference substance; A_s is the integrated value of the differential heat flow when the measuring vessel contains the sample; A_{sapp} is the integrated value of the differential heat flow when the measuring vessel contains the reference substance; and A_E is the integrated value of differential heat flow in the case when the measuring vessel is empty. The temperature dependence of heat capacity for all studied substances was approximately linear. Thus, the average heat capacity over individual temperature steps can be considered as a true heat capacity relating to the mean temperature of the interval. The correction for sample vaporization as discussed in Zábranský et al.[26] was not applied. This is because the *pVT* ($V_m^{(s)} = f(T)$) data for solid tetracene and pentacene needed for the correction are not available. Moreover, the sublimation and vapor pressures of these compounds are low. For example, the vapor pressures of tetracene and pentacene at 600 K are 5.8 kPa and 77 Pa, respectively, as estimated from the vapor pressure data reported by de Kruif.[27] Any correction made would be much smaller than the experimental uncertainty of our measurements themselves and can be neglected. The correction does not exceed 0.1 % even for much more volatile compounds where the volume of the condensed phase is about 3/4 of the total volume of the measuring cell.[18,28] The saturated molar heat capacities C_{sat} obtained in this work are identical to isobaric molar heat capacities C_p in the temperature range studied as it is not necessary to make a clear distinction between C_p along the saturation curve and C_{sat} below 0.9 T_b, where T_b is the normal boiling temperature.[26]

In addition to the measurements performed using the step method, we performed experiments using the continuous method in the temperature range (173 to 673) K to investigate phase transitions and thermal stability. The measurements were performed with a heating rate of 5 K·min^{-1}. Peak areas were integrated using the Setaram software package SetSoft 2000. General principles for peak evaluations can be found in Höhne et al.[17]

Results and Discussion

Tetracene Calorimetric Data and Data Evaluation. A DSC thermogram and apparent heat capacities for tetracene are shown in Figure 1A and B, respectively. Two solid−solid transitions were detected in the temperature range (173 to 673) K. The temperatures and enthalpies associated with the solid−solid transitions and the temperature and enthalpy of fusion for tetracene are given in Table 1. The values in Table 1 are the means of triplicate experiments with fresh samples. The reported uncertainties are twice the estimated standard deviations of the mean (95 % confidence interval, coverage factor $k = 2$). Our values are in good agreement with the cited literature as shown in Table 1. The table does not include all T_{fus} values reported in the literature. Only references reporting physicochemical property measurements are presented. To our knowledge, the phase transition at (398.1 ± 1.2) K is not reported in the literature. Successive calorimetric scans repeated with the same sample clearly indicate that tetracene decomposes upon melting at ≈ 626 K.

Heat capacity values obtained at both laboratories, reported in Table 2, are in close agreement in the temperature interval where the measurements overlap. For tetracene, the heat capacity data for the crystalline phases are reported only up to $T = 558$ K. The vicinity of the crystal II to crystal I transition and the melting process did not allow us to determine the heat capacity for crystal phase I. The heat capacity data for the liquid phase presented in Table 2 are affected by tetracene decomposition upon melting.

Pentacene Calorimetric Data and Data Evaluation. As can be seen in the thermogram (Figure 2A) pentacene decomposes at ≈ 635 K when heated with a heating rate of 5 K·min^{-1} under an argon atmosphere. During the measurements performed using the step method, pentacene became thermally unstable at approximately 600 K (Figure 2B). These values are both consistent with published decomposition temperatures for pentacene which range from (592 to 633) K.[29,30] There is no evidence of phase transitions at lower temperatures, and the reported melting temperature for pentacene, 544 K,[31] is clearly in error. Again, the heat capacity values obtained at both laboratories, also reported in Table 2, are in close agreement in the temperature interval where the measurements overlap. Pentacene heat capacities are reported up to $T = 600$ K above which decomposition was observed.

Heat Capacity Correlation and Prediction. The experimental isobaric molar heat capacities for solid tetracene and pentacene were fit with a polynomial expression, eq 2, using the weighted least-squares method

$$C_p/(\mathrm{J\cdot K^{-1}\cdot mol^{-1}}) = A_0 + A_1(T/\mathrm{K}) + A_2(T/\mathrm{K})^2 \quad (2)$$

The points were weighted according to their experimental uncertainties. The weighting factor was represented by the variance of the measured data. The parameters A_0, A_1, and A_2 together with the standard deviations of the fit, σ, are given in Table 3.

Table 3. Parameters A_0, A_1, and A_2 of Equation 2 and Standard Deviations of the Fit σ[a]

		parameters			temperature range		
compound	phase	A_0	A_1	$A_2 \cdot 10^4$	T_{min}/K	T_{max}/K	σ/(J·K^{-1}·mol^{-1})
tetracene	crystal III	−91.69908	1.42133	−8.2	258	389	1.3
tetracene	crystal II	−4.48770	0.88587	0	409	558	1.9
tetracene	liquid[b]	237.00895	0.41428	0	647	667	0.004
pentacene	crystal	−93.80415	1.57206	−7.2	258	598	2.9

[a] $\sigma = [\sum_{i=1}^{n} (C_p - C_p^{calcd})_i^2/(n - m)]^{1/2}$, where n is the number of fitted data points and m is the number of adjustable parameters. [b] Tetracene decomposes on melting.

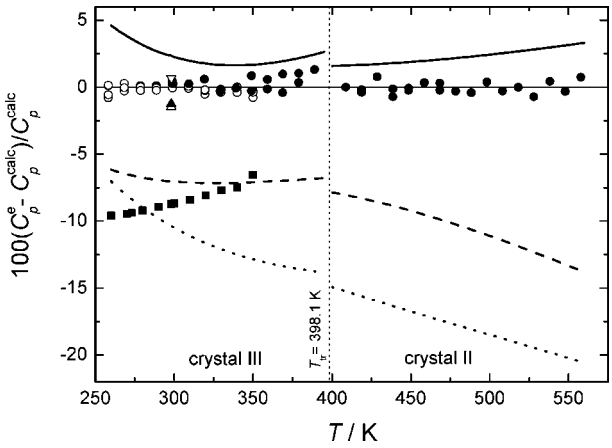

Figure 3. Deviation of experimental and estimated heat capacities for solid tetracene C_p^e from values C_p^{calcd} calculated from eq 2 using the parameters listed in Table 3. ○, this work (Micro DSC III); ●, this work (TG-DSC 111); ■, Wong and Westrum;[4] △, group contribution method by Domalski and Hearing (298.15 K);[6] ▽, group contribution method by Chickos et al. (298.15 K);[9] ▲, group contribution method by Richard and Helgeson (298.15 K);[8] —, predictive semiempirical correlation by Laštovka and Shaw;[12] •••, partition function method by Goodman et al.;[10] - - -, isochoric molar heat capacity C_V calculated by DFT.

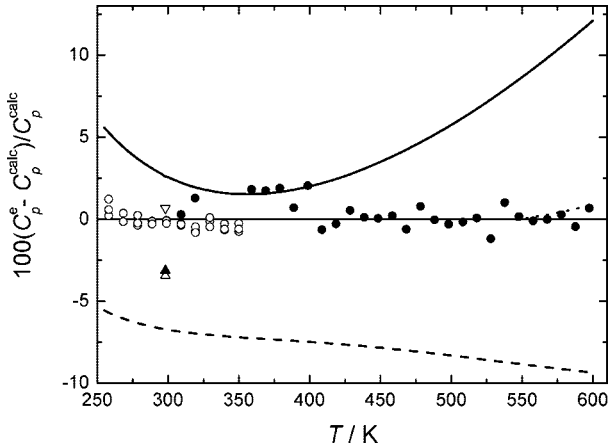

Figure 4. Deviation of experimental and estimated heat capacities for solid pentacene C_p^e from values C_p^{calcd} calculated from eq 2 using the parameters listed in Table 3. ○, this work (Micro DSC III); ●, this work (TG-DSC 111); •••, Durupt et al.[33] (the data were misattributed to liquid); △, group contribution method by Domalski and Hearing (298.15 K);[6] ▽, group contribution method by Chickos et al. (298.15 K);[9] ▲, group contribution method by Richard and Helgeson (298.15 K);[8] —, predictive semiempirical correlation by Laštovka and Shaw;[12] - - -, isochoric molar heat capacity C_V calculated by DFT.

Comparisons between the heat capacity data for tetracene and pentacene obtained in this work with data and estimates from the literature are presented in Figures 3 and 4, respectively. The values of the heat capacity of tetracene published by Wong and Westrum[4] are lower than those obtained in this work and differ significantly from predicted

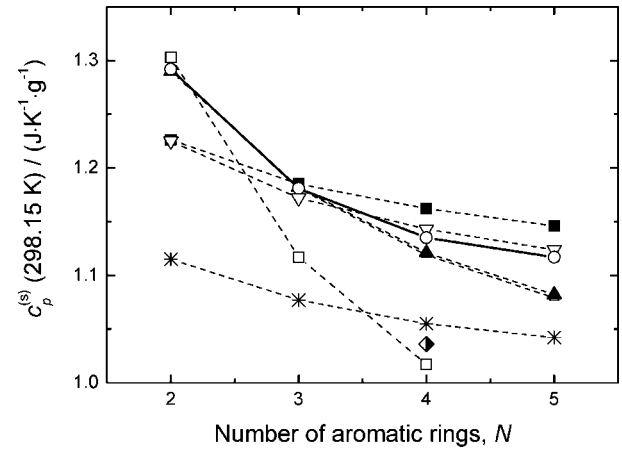

Figure 5. Experimental and estimated specific heat capacities $c_p^{(s)}$ for linear PAHs at $T = 298.15$ K. -○-, experimental heat capacity (naphthalene ($N = 2$),[24] anthracene ($N = 3$),[36] tetracene ($N = 4$), and pentacene ($N = 5$), this work); half-filled diamond, experimental value for tetracene reported by Wong and Westrum;[4] --Δ--, group contribution method by Domalski and Hearing;[6] --∇--, group contribution method by Chickos et al. (298.15 K);[9] --▲--, group contribution method by Richard and Helgeson;[8] --■--, predictive semiempirical correlation by Laštovka and Shaw;[12] --□--, partition function method by Goodman et al.;[10] --*--, isochoric specific heat capacity c_V calculated by DFT.

values. Their data are clearly in error. The differences vary from (20 to 23) J·mol^{-1}·K^{-1} (relative deviations from (6.5 to 9.6 %)), while values estimated using group contribution methods for $C_p^{(s)}$ at $T = 298.15$ K suggested by Domalski and Hearing,[6] Chickos et al.,[9] and Richard and Helgeson[8] differ by 1.5 %, 0.7 %, and 1.3 %, respectively, from our data. We note that heat capacity data for tetracene reported by Wong and Westrum[4] were not used in the development of either of these group contribution methods. The partition function from Goodman et al.[10] significantly underestimates $C_p^{(s)}$ and diverges from the experimental data as temperature increases. The DFT based C_V calculations underestimate the new experimental $C_p^{(s)}$ values as expected but overestimate values from Wong and Westrum.[4] It was this overestimation that led to the current study, as it was inconsistent with expectations. The correlation developed by Laštovka and Shaw[12,13,32] overpredicts $C_p^{(s)}$ but provides good predictions over the entire experimental temperature range (258 to 558) K. The maximum deviation is less than 5 %, and the average deviation is less than 2 %. For pentacene, the results are similar, although the deviations are somewhat larger on average. Values estimated using group contribution methods for $C_p^{(s)}$ at $T = 298.15$ K suggested by Domalski and Hearing,[6] Chickos et al.,[9] and Richard and Helgeson[8] differ by 3.4 %, 0.6 %, and 3.1 %, respectively. The partition function from Goodman et al.[10] could not be applied as the radius of gyration is not available for pentacene. Again, the DFT-based C_V calculations underestimate the new experimental $C_p^{(s)}$ values, as expected, but remain within 10 % of the data. The

predictive correlation developed by Laštovka and Shaw[12,13,32] overpredicts $C_p^{(s)}$. The maximum deviation is less than 5 %, at temperatures less than 550 K, and the average deviation is less than 3 %. The correlation diverges at higher temperatures, and the error is 15 % at 600 K. This divergence may reflect a deficiency in the correlation or it could be linked to the slow initial, exothermic decomposition of the pentacene. The effect is subtle. Experimental heat capacity data for pentacene reported by Durupt et al.,[33] which are in good agreement with the solid state heat capacities reported here (the deviation is less than 0.8 %), were misattributed to liquid in the temperature interval (546 to 594) K. We note that the authors developed the group contribution method for heat capacities of liquid heavy aromatics based on these data.

Heat Capacity Trends for Linear PAHs. $C_p^{(s)}$ data and calculations presented here facilitate the observation and prediction of trends with the number of rings for linear PAHs. As these are more evident on a unit mass basis, specific heat capacity values, $c_p^{(s)}$, at $T = 298.15$ K, are presented in Figure 5, as a function of the number of aromatic rings in the compounds. The bounds and asymptotic behavior for $c_p^{(s)}$ are clearly evident.

Conclusions

Solid state heat capacity data for tetracene and pentacene are reported in the temperature range (258 to 600) K. The new heat capacity data and prediction results show that previously reported heat capacity data for solid tetracene are in error. A previously unreported solid−solid phase transition for tetracene, at $T = 398.1$ K, was observed. The transition temperatures and enthalpies for a second solid−solid transition and the solid−liquid transition were found to be in agreement with the literature. Tetracene decomposes on melting, while pentacene decomposes before melting. The previously reported melting temperature for pentacene is not supported.

Literature Cited

(1) Murgich, J.; Abanero, J. A.; Strausz, O. P. Molecular recognition in aggregates formed by asphaltene and resin molecules from the Athabasca oil sand. *Energy Fuels* **1999**, *13*, 278–286.

(2) Leon, O.; Rogel, E.; Espidel, J.; Torres, G. Asphaltenes: Structural characterization, self-association, and stability behavior. *Energy Fuels* **2000**, *14*, 6–10.

(3) Sallamie, N.; Shaw, J. M. Heat capacity prediction for polynuclear aromatic solids using vibration spectra. *Fluid Phase Equilib.* **2005**, *237*, 100–110.

(4) Wong, W. K.; Westrum, E. F. Thermodynamics of Polynuclear Aromatic-Molecules:II. Low-Temperature Thermal-Properties of Perylene, Coronene, and Naphthacene. *Mol. Cryst. Liq. Cryst.* **1980**, *61*, 207–228.

(5) Michaelian, K. H.; Billinghurst, B. E.; Shaw, J. M.; Laštovka, V. Far-infrared Photoacoustic Spectra of Tetracene, Pentacene, Perylene and Pyrene. *Vib. Spectrosc.* **2008**, doi:10.1016/j.vibspec.2008.04.005.

(6) Domalski, E. S.; Hearing, E. D. Estimation of the Thermodynamic Properties of Hydrocarbons at 298.15 K. *J. Phys. Chem. Ref. Data* **1988**, *17*, 1637–1678.

(7) Benson, S. W.; Buss, J. H. Additivity Rules for the Estimation of Molecular Properties - Thermodynamic Properties. *J. Chem. Phys.* **1958**, *29*, 546–572.

(8) Richard, L.; Helgeson, H. C. Calculation of the thermodynamic properties at elevated temperatures and pressures of saturated and aromatic high molecular weight solid and liquid hydrocarbons in kerogen, bitumen, petroleum, and other organic matter of biogeochemical interest. *Geochim. Cosmochim. Acta* **1998**, *62*, 3591–3636.

(9) Chickos, J. S.; Hesse, D. G.; Liebman, J. F. A Group Additivity Approach for the Estimation of Heat-Capacities of Organic Liquids and Solids at 298 K. *Struct. Chem.* **1993**, *4*, 261–269.

(10) Goodman, B. T.; Wilding, W. V.; Oscarson, J. L.; Rowley, R. L. Use of the DIPPR Database for Development of Quantitative Structure-Property Relationship Correlations: Heat Capacity of Solid Organic Compounds. *J. Chem. Eng. Data* **2004**, *49*, 24–31.

(11) Joback, K. G.; Reid, R. C. Estimation of pure-component properties from group-contributions. *Chem. Eng. Commun.* **1987**, *57*, 233–243.

(12) Laštovka, V.; Shaw, J. M. Predictive Correlation for C_p of Organic Solids Based on Elemental Composition. *J. Chem. Eng. Data* **2007**, *52*, 1160–1164.

(13) Laštovka, V.; Fulem, M.; Becerra, M.; Shaw, J. M. A similarity variable for estimating the heat capacity of solid organic compounds Part II. Application: Heat capacity calculation for ill-defined organic solids. *Fluid Phase Equilib.* **2008**, *268*, 134–141.

(14) Frisch, M. J. ; Trucks, G. W.; Schlegel, H. B.; Scuseria, G. E.; Robb, M. A.; Cheeseman, J. R.; Montgomery, J., J. A.; Vreven, T.; Kudin, K. N.; Burant, J. C.; Millam, J. M.; Iyengar, S. S.; Tomasi, J.; Barone, V.; Mennucci, B.; Cossi, M.; Scalmani, G.; Rega, N.; Petersson, G. A.; Nakatsuji, H.; Hada, M.; Ehara, M.; Toyota, K.; Fukuda, R.; Hasegawa, J.; Ishida, M.; Nakajima, T.; Honda, Y.; Kitao, O.; Nakai, H.; Klene, M.; Li, X.; Knox, J. E.; Hratchian, H. P.; Cross, J. B.; Bakken, V.; Adamo, C.; Jaramillo, J.; Gomperts, R.; Stratmann, R. E.; Yazyev, O.; Austin, A. J.; Cammi, R.; Pomelli, C.; Ochterski, J. W.; Ayala, P. Y.; Morokuma, K.; Voth, G. A.; Salvador, P.; Dannenberg, J. J.; Zakrzewski, V. G.; Dapprich, S.; Daniels, A. D.; Strain, M. C.; Farkas, O.; Malick, D. K.; Rabuck, A. D.; Raghavachari, K.; Foresman, J. B.; Ortiz, J. V.; Cui, Q.; Baboul, A. G.; Clifford, S.; Cioslowski, J.; Stefanov, B. B.; Liu, G.; Liashenko, A.; Piskorz, P.; Komaromi, I.; Martin, R. L.; Fox, D. J.; Keith, T.; Al-Laham, M. A.; Peng, C. Y.; Nanayakkara, A.; Challacombe, M.; Gill, P. M. W.; Johnson, B.; Chen, W.; Wong, M. W.; Gonzalez, C.; Pople, J. A. *Gaussian 03, revision C.02*, Gaussian, Inc.: Wallingford CT, 2004.

(15) Becke, A. D. Density-Functional Thermochemistry. 3. The Role of Exact Exchange. *J. Chem. Phys.* **1993**, *98*, 5648–5652.

(16) Lee, C. T.; Yang, W. T.; Parr, R. G. Development of the Colle-Salvetti Correlation-Energy Formula into a Functional of the Electron-Density. *Phys. Rev. B* **1988**, *37*, 785–789.

(17) Höhne, G. W. H.; Hemminger, W. F.; Flammersheim, H.-J. *Differential Scanning Calorimetry*, 2nd ed.; Springer Verlag: Berlin, 2003.

(18) Straka, M.; Růžička, K.; Růžička, V. Heat capacities of chloroanilines and chloronitrobenzenes. *J. Chem. Eng. Data* **2007**, *52*, 1375–1380.

(19) Cammenga, H. K.; Eysel, W.; Gmelin, E.; Hemminger, W.; Höhne, G. W. H.; Sarge, S. M. The Temperature Calibration of Scanning Calorimeters. 2. Calibration Substances. *Thermochim. Acta* **1993**, *219*, 333–342.

(20) Höhne, G. W. H.; Cammenga, H. K.; Eysel, W.; Gmelin, E.; Hemminger, W. The Temperature Calibration of Scanning Calorimeters. *Thermochim. Acta* **1990**, *160*, 1–12.

(21) Sarge, S. M.; Gmelin, E.; Höhne, G. W. H.; Cammenga, H. K.; Hemminger, W.; Eysel, W. The Caloric Calibration of Scanning Calorimeters. *Thermochim. Acta* **1994**, *247*, 129–168.

(22) Sarge, S. M.; Hemminger, W.; Gmelin, E.; Höhne, G. W. H.; Cammenga, H. K.; Eysel, W. Metrologically based procedures for the temperature, heat and heat flow rate calibration of DSC. *J. Therm. Anal.* **1997**, *49*, 1125–1134.

(23) Sabbah, R.; Xu-wu, A.; Chickos, J. S.; Planas Leitao, M. L.; Roux, M. V.; Torres, L. A. Reference materials for calorimetry and differential thermal analysis. *Thermochim. Acta* **1999**, *331*, 93–204.

(24) Chirico, R. D.; Knipmeyer, S. E.; Steele, W. V. Heat capacities, enthalpy increments, and derived thermodynamic functions for naphthalene between the temperatures 5 and 440 K. *J. Chem. Thermodyn.* **2002**, *34*, 1873–1884.

(25) Finke, H. L.; Messerly, J. F.; Lee, S. H.; Osborn, A. G.; Douslin, D. R. Comprehensive Thermodynamic Studies of Seven Aromatic-Hydrocarbons. *J. Chem. Thermodyn.* **1977**, *9*, 937–956.

(26) Zábranský, M.; Růžička, V.; Majer, V.; Domalski, E. S. Heat Capacity of Liquids. Critical Review and Recommended Values. *J. Phys. Chem. Ref. Data*, Monograph No. 6; American Chemical Society: Washington, DC, 1996.

(27) de Kruif, C. G. Enthalpies of Sublimation and Vapor-Pressures of 11 Polycyclic-Hydrocarbons. *J. Chem. Thermodyn.* **1980**, *12*, 243–248.

(28) Čenský, M.; Lipovská, M.; Schmidt, H. G.; Růžička, V.; Wolf, G. Heat capacities of hydroxy and aminoderivatives of benzene. *J. Therm. Anal. Calorim.* **2001**, *63*, 879–899.

(29) Chen, K. Y.; Hsieh, H. H.; Wu, C. C.; Hwang, J. J.; Chow, T. J. A new type of soluble pentacene precursor for organic thin-film transistors. *Chem. Commun.* **2007**, 1065–1067.

(30) Merlo, J. A.; Newman, C. R.; Gerlach, C. P.; Kelley, T. W.; Muyres, D. V.; Fritz, S. E.; Toney, M. F.; Frisbie, C. D. p-Channel organic semiconductors based on hybrid acene-thiophene molecules for thin-film transistor applications. *J. Am. Chem. Soc.* **2005**, *127*, 3997–4009.

(31) Linstrom, P. J., Mallard, W. G., Eds.; *NIST Chemistry WebBook*, NIST Standard Reference Database Number 69; National Institute of Standards and Technology: Gaithersburg MD, 20899 (http://webbook.nist.gov), 2005.

(32) Laštovka, V.; Sallamie, N.; Shaw, J. M. A similarity variable for estimating the heat capacity of solid organic compounds Part I. Fundamentals. *Fluid Phase Equilib.* **2008**, *268*, 51–60.

(33) Durupt, N.; Aoulmi, A.; Bouroukba, M.; Rogalski, M. Heat-Capacities of Liquid Polycyclic Aromatic-Hydrocarbons. *Thermochim. Acta* **1995**, *260*, 87–94.
(34) Nagano, Y. Standard enthalpies of formation of phenanthrene and naphthacene. *J. Chem. Thermodyn.* **2002**, *34*, 377–383.
(35) Wakayama, N.; Inokuchi, H. Heats of Sublimation of Polycyclic Aromatic Hydrocarbons and Their Molecular Packings. *Bull. Chem. Soc. Jpn.* **1967**, *40*, 2267–2271.
(36) Goursot, P.; Girdhar, H. L.; Westrum, E. F. Thermodynamics of polynuclear aromatic molecules. 3. Heat capacities and enthalpies of fusion of anthracene. *J. Phys. Chem.* **1970**, *74*, 2538–2541.

Received for review May 28, 2008. Accepted July 14, 2008. This research was supported by the Alberta Energy Research Institute, ConocoPhillips, Inc., Imperial Oil Resources, Halliburton, Kellogg Brown and Root, NEXEN Inc., Shell Canada, Total, and the Natural Science and Engineering Research Council (NSERC). This work was also supported by the Ministry of Education of the Czech Republic under grant MSM 604 613 7307.

JE800382B